Heating Mechanisms in Short-Pulse Laser-Driven Cone Targets

R. J. Mason*

Applied Physics Division, Los Alamos National Laboratory, Los Alamos, New Mexico 87545, USA

(Received 20 September 2005; published 23 January 2006)

The fast ignitor is a modern approach to laser fusion that uses a short-pulse laser to initiate thermonuclear burn. In its simplest form the laser launches relativistic electrons that carry its energy to a precompressed fusion target. Cones have been used to give the light access to the dense target core through the low-density ablative cloud surrounding it. Here the ANTHEM implicit hybrid simulation model shows that the peak ion temperatures measured in recent cone target experiments arose chiefly from return current joule heating, mildly supplemented by relativistic electron drag. Magnetic fields augment this heating only slightly, but capture hot electrons near the cone surface and force the hot electron stream into filaments.

DOI: 10.1103/PhysRevLett.96.035001 PACS numbers: 52.57.Kk, 52.65.Rr

The fast ignitor approach [1] to laser fusion first compresses a fusion target to 100 g/cm^3 densities with nanosecond time scale laser pulses, and then heats the surface of a compressed target core with either ions or relativistic electrons launched by a subsequent picosecond laser pulse. The scheme was first proposed to avoid the extreme densities and pulse shaping requirements demanded, for example, in compressing shells [2] for central hot-spot ignition [3]. Cones have been used with hot electron fast ignition to help channel the short-pulse light through the low density surrounding blowoff plasma to the vicinity of the core. At ILE, Kodama *et al.* [4] have compressed carbon-deuterium (CD) shells with reentrant cones to core densities of 100 g/cm^3 and subsequently heated the target cores to temperatures exceeding 800 eV with a 300 J, 1.06 μm picosecond laser beam. At LLE, Rochester researchers have verified the high compression of cone target cores under both direct and indirect drive [5]. In this Letter we apply the 2D simulation code ANTHEM [6] to cone targets. We characterize the dominant laser-target transport interactions, replicate the core temperatures experimentally achieved, and suggest system changes to improve hot electron coupling to target cores.

The problem.—We first discuss the canonical target of Fig. 1. A plastic CD shell has been precompressed into a 100 gm/cm^3 (1.8×10^{25} electrons/cm^3) superdense core at 400 eV by a conventional nanosecond laser system. An ablative CD cloud surrounds it, decaying exponentially from 1/50 of the peak core density—typical of an ablation front density—down to an arbitrary $10^{22} e^-$/cm^3 some 50 μm from the core center. The cloud is penetrated on the left by a single hollow simulated gold cone with walls here at a 20° angle, and possessing a peak electron density of 1.5×10^{24} (for ionization $Z = 30$). The cone has a flattened tip, 36 μm wide. Its walls and tip are taken as 6 μm thick. The sides of the tip are steep with a 5 μm scale length. The cone tip is separated from the core by 15 μm. The incident 1.06 μm short laser pulse rises to peak intensity $I = 10^{19}$ W/cm^2 over 10 fs (for computational economy), and is constant thereafter. Spatially, the beam is taken as flat at the cone tip. Light enters along the central cone axis.

The model.—We simulate the interactions with the 2D implicit hybrid simulation code ANTHEM [6]. Here, the code treats the target and its surroundings as separate ion and cold electron Eulerian fluids, each with inertia. The cold electrons scatter off the ions, and undergo joule heating, flux-limited ($f = 0.05$) thermal conduction, and thermal exchange with the ions. Hot electrons are treated as relativistically collisional, mass-weighted particle-in-cell (PIC) particles. The three plasma components are also coupled together by self-consistent E and B fields computed via the implicit moment method [7]. Laser light is propagated to the critical surface (where the light frequency ω equals the relativistic plasma frequency ω_p')

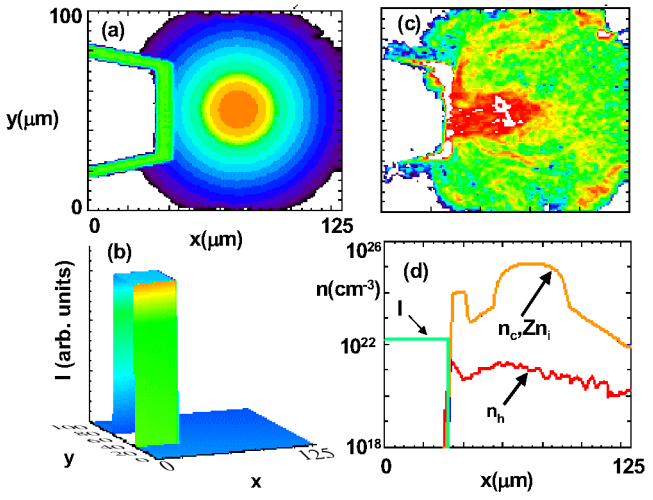

FIG. 1 (color online). (a) Contours of cold density n_c in our cone targets, and (b) the laser intensity I (arbitrary units) depositing on the cone inner (left) surface. (c) Hot electron density, n_h contours at 1.08 ps, and (d) central ($y = 50$ μm) cuts for n_h, n_c, and Zn_i (cm^{-3}) and I (arbitrary units).

via a grid-following algorithm that is typical of traditional inertial confinement fusion hydrodynamics codes. At critical, a fraction of the energy, 40% [4], is absorbed, and a corresponding fraction of the cold electrons is converted into the PIC hot electron particles emitted in a 22.5° beam toward the core at temperatures T_h obeying plane wave ponderomotive scaling [8]; at 10^{19} W/cm^2 this give a relativistic γ_h of 2.1, and $T_h = 0.6$ MeV. The remaining light is reflected. All the light pushes on the surrounding plasma with a density-limited [9] ponderomotive force determined from the local intensity gradient. With implicit hybrid simulation we employ 0.1 fs time steps and 1.0 μm spatial cells for our simulations, while still avoiding the numerical instabilities requiring much finer resolution with traditional PIC simulation. Recently, ANTHEM was used to show that spontaneous B fields arise at steep density interfaces and retain electrons [9] near the surface of dense foils. Others have used the alternate large scale plasma (LSP) implicit scheme [10] to model the ILE short-pulse–CD-core interaction, but its modeling lacked the actual presence of the cone and its steep density interface, and used no grid-following laser package, but deposited laser energy as an electron beam [11] at the edge of the coronal cloud locally mixed with gold ions. The collision models in LSP were classical.

Results.—Figure 1(a) shows the overall target configuration with the cold background density peaking near $x = 75$ μm, and with the cone on the left. Figure 1(b) is a surface plot of the laser intensity I (arbitrary units) entering the cone. Figures 1(c) and 1(d) show 1.08 ps code output pictures of hot electrons (density n_h) flowing from the cone tip into the compressed core and its surrounding ablative cloud. The highest density ($4 \times 10^{21} e^-/\text{cm}^3$) of "hots" occurs on the laser-facing surface of the tip. This exceeds classical critical ($n_{\text{crt}} = 10^{21} e^-/\text{cm}^3$) due to the relativistic alteration of the electron mass, as well as the magnetic surface retention [9] of emitted hots. The hot density drops away from the cone to 8×10^{20} cm^{-3}, then rises again as the core is entered, reaching $2 \times 10^{21} e^-/\text{cm}^3$ near its left edge. In Fig. 1(a) we see that the hot density stream has broken into filaments, identified in Ref. [9] as due to an interaction of B fields and background resistivity. Associated magnetic filaments are evident in the core near $x = 65$ μm, Figs. 2(c) and 2(d), but these are only at the 30 MG level as compared to the 300 MG thermoelectric fields seen at the cone surface. The LSP calculation could see no such surface fields, since the steep density gradients near an actual cone were missing.

The most pronounced cold heating takes place throughout the lower density cloud outside the core where cold electrons are replaced by hots and pulled to nearly relativistic return speeds to maintain quasineutrality. Thus, a bath of heated background electrons rapidly surrounds the cold core. This is evident in Fig. 2(b) where cold electron temperatures—well beyond a kilovolt - are seen for $x <$

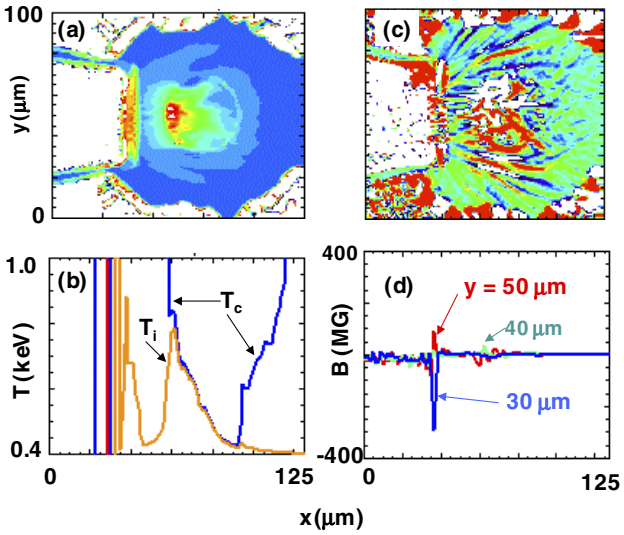

FIG. 2 (color online). (a) Ion temperature contours reaching 770 eV at 1.14 ps in the central crescent, and calibrated in (b) with T_c higher in the outer cloud. Corresponding B-field contours (c) with core filaments, and cone values reaching 300 MG recorded in (d).

60 and >100 μm. This has little immediate conductive influence on cold electrons in the core, however, because of the great disparity of core and coronal densities. Cloud ions acquire some collisional heating from the colds, but the coupling rate is low at cloud densities. Direct shock heating of the ions occurs near the cone tip. However, most significant for neutron production inside the core is the high ion temperature $T_i \sim 770$ eV, peaking the temperature profile near $x = 60$ μm in a crescent [Fig. 2(a)] centered toward the cone and approximating the experimental results [4]. How does this temperature spike arise?

The LSP simulations [10] attributed high core temperature in cone targets [4] to magnetic stopping. To the contrary, we find that when the magnetic field is suppressed by going to the electrostatic limit [9] in our simulations the peak temperature still reaches 710 eV by 1.12 ps, and 800 eV by 1.5 ps. Electrostatic E fields are obtained for ANTHEM by setting $B = 0$, suppressing Faraday's Law, and using the implicit current correction [6] to guarantee that $\nabla \cdot \mathbf{E}$ tracks the total charge. An alternate test, setting $\boldsymbol{v} \times \boldsymbol{B} = 0$ throughout, gave essentially the same result. In Fig. 2 the high T_i arises chiefly from joule heating. If the cold electron-ion scattering rate ν_{ei} determining resistivity η for joule heating is set to zero, the core electron temperature T_c reaches only to 450 eV by 1.0 ps. The residual 50 eV increase comes directly from hot electron energy drag deposition into the colds. Also, the core ions remain at the original 400 eV, since the cold electron-ion energy coupling rate R_{ei} is proportional to ν_{ei} [1].

For this high-density short-pulse environment the various collision rates, scatter, drag, etc., are all somewhat controversial. Consequently, as additional tests we sought to determine dependency of the peak ion temperature on

these rates. When, for example, ν_{ei} is increased by a factor of 3, we find that the peak ion temperature at 1.1 ps rises to 1.1 keV. Alternatively, if ν_{ei} is reduced by 3 (with R_{ei} held constant) the maximum T_i achieved is only 600 eV. Finally, when the resistivity is unchanged but the coupling rate R_{ei} is multiplied threefold, the peak T_i rises modestly from the original 770 eV to 810 eV.

Deposition from drag of the hot electrons against the cold electron background was originally proposed as the chief mechanism for fuel heating under electron fast ignition [1]. We use relativistic range formulas from Jackson [12]. For our Fig. 1 conditions the resultant range appears to be 60 μm. If, however, the drag rate can be multiplied by a factor of 3, the peak T_i rises to 1.0 keV at 1 ps. We note that lowering the core density by a factor of 5 (for a peak 20 g/cm^3 and $3.6 \times 10^{24} e^-/\mathrm{cm}^3$) makes no significant increase in the ion temperatures achieved, since both the drag and scattering rates decrease in proportion to the background density.

Figure 3(a) shows the hot electron phase space at 387 fs with the accumulated density weights of all the particles vs their x positions and super velocities $u_x = v_{xh}\gamma_h$. The electrons are launched at the cone tip at $x = 35$ μm near $u_h = 3c$ and slow in the $x = 65$ μm core region. Figure 3(b) shows that there is a corresponding retarding E field reaching 0.03 MeV/μm. This field varies slowly and is 10 times smaller after $t = 750$ fs partly due to a resistance decrease with background heating. A much higher fluctuating E field is evident near the cone surface. Most of the hots continue on, moving to the right to the edge of the cloud, and these are also slowed, but less dramatically, by E fields pulling in the background "colds." Some of the hots are reflected and returned from the rear of the core and a vertical accumulation of electrons and a bright spot near the core tip indicates hot electron surface retention. Going more deeply in x, the beam in phase space rapidly decelerates and then disappears due to full absorption into the colds. Vector flux plots [not included here] at 1.1 ps of the hot and cold electron streams for the Fig. 1 problem show fluxes filling the whole cloud volume out to the right, $x = 125$ μm edge of the test area where hot electrons absorb and colds return. The fluxes are most intense near the cone tip.

Results obtained with the magnetic field suppressed are collected in Fig. 4. Without B field the peak T_i drops only a little to 710 eV by 1.12 ps, as previously indicated, and the region of heating remains a crescent with its bottom facing the laser. This test clearly shows that the main core heating cannot be attributed to "magnetic stopping" [10]. Without B fields the uniformity of heating and the size of the peak heated region are much greater. Generally, B fields make the core heating process more difficult. First, thermoelectric B fields retain [9] the hot electrons near the spot, reducing the density of hots n_h flowing toward the core. Also, the B fields lead to resistive Weibel instability inside the cloud and filamentation [9], as well as random deflection of flux from the core. Sentoku [13] points to a Weibel-like mechanism for low-density heating, and this may well prevail in the corona. However, this scales as B/ω_p^2, making it too weak for significance in the core. The resistive E field slowing in Fig. 3(a) significantly diminishes after 650 fs when higher T_c decreases the Spitzer ν_{ei}. Use of a

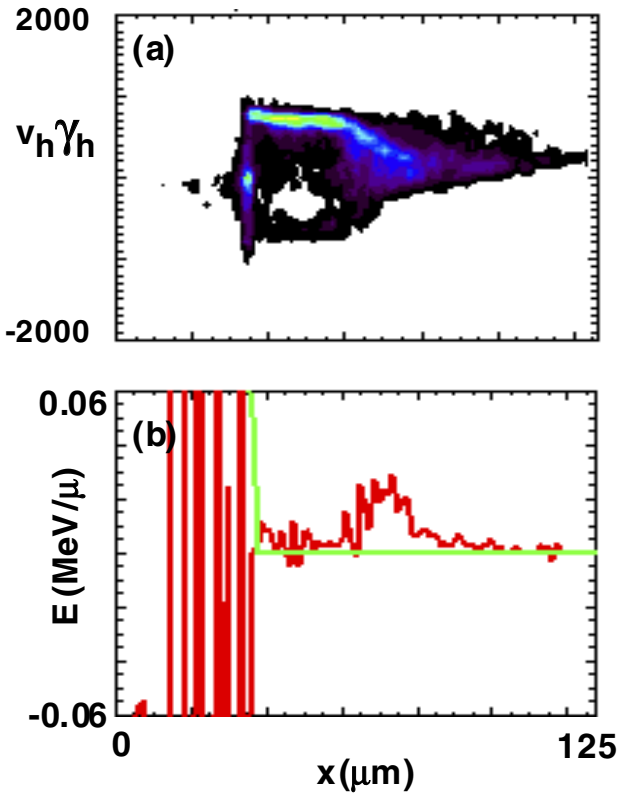

FIG. 3 (color online). (a) Hot electrons in phase space at 387 fs with electrons slowed by resistive E fields (b) beyond $x = 60$ μm.

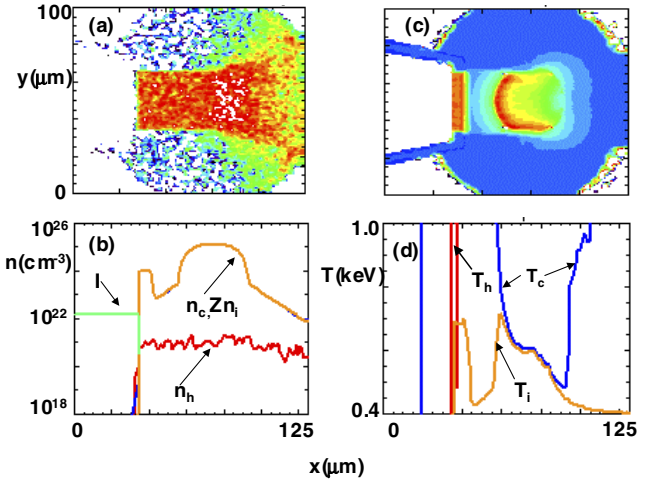

FIG. 4 (color online). Hot electron density (a) and (b) at 1.1 ps with B field suppressed, and (c) corresponding ion temperature contours and calibration (d).

finer mesh might alter our conclusions. However, ANTHEM tests with a 20-fold smaller mesh (and smaller core) in each direction (i.e. $\Delta x = \Delta y = 0.05$ μm) replicated the present results.

We have employed a broad, flat laser spot to minimize B field surface retention and optimize n_h penetration [14] of the cloud. Even so, with the passage of time thermoelectric B fields drift onto the cone tip from its walls. There they develop randomly at the 300 MG level from density variations in the hot particle emission and cause surface retention. If alternatively, we impose a much smaller, Gaussian laser spot with a 14 μm FWHM, then the hot penetration is much reduced in the fashion of the Ref. [9] foil runs, and violent streamers are emitted from the center of the spot. Consequently, with this smaller spot at 1.1 ps the peak core temperature runs no higher than 550 eV.

What is the optimum cone-core separation distance? This could not be gleaned with LSP, since the actual cone was missing. Here we have used $\sim$15 μm. In another simulation, we reduced this distance to zero, pushing the cone right against the steep portion (1/50 peak density point) of the core. This failed to improve the heating; the peak T_i reached only 670 eV at 1.0 ps. Alternatively, we increased the cone-core separation distance to 30 μm. This introduced a potential barrier to hot penetration. Where it meets the cone, our exponentially decaying cloud then drops to a minimum density of only $10^{22} e^-/\mathrm{cm}^3$. With magnetic retention functioning, the hot electron density at times exceeds this minimum. Consequently, the outgoing hot electron flux cannot draw a free return current, and cannot fully pass beyond the minimum. So in the core at 1.1 ps with the larger separation, the peak T_i goes no higher than 550 eV. Our original separation of 15 μm was somewhat of an optimum.

Certainly, higher core temperatures should come with higher laser intensity I. Our simulations confirm this. By ponderomotive scaling the Lorentz factor for hots varies as $\gamma_h \sim I^{1/2}$. The electrons nearly all move at the speed c. So, in a given time interval Δt (and for high energies) to carry away energy $I\Delta t$, the density of emitted hot will scale roughly as $n_h \sim I^{1/2}$. Higher intensities will yield a higher input hot flux, and correspondingly a higher return flux with greater joule heating. Moreover, the more energetic electrons are ''stiffer,'' i.e., less easily deflected by fluctuating B fields into filaments that miss the core. Accordingly, in additional simulations setting $I = 2 \times 10^{19}$ W/cm^2 the peak T_i rose to 860 eV, while for $I = 4 \times 10^{19}$ W/cm^2 a core temperature of 1.1 keV was achieved. On the other hand, higher γ_h raises the hot electron range and reduces that portion of heating that can come from direct drag deposition.

Finally, what are the possible benefits of shorter wavelength for the short-pulse illumination? For our Fig. 1 configuration 0.25 μm is too short. The hot electrons have a γ_h of only 1.17 for a T_h of 52 keV. A 16-fold higher density n_h is generated, but at 10^{19} W/cm^2 the hot electron flux is absorbed before it reaches the core. On the other hand, a switch to green short-pulse light at 0.5 μm does slightly improve the coupling; T_i reaches 810 eV at 1 ps. The optimal tuning of the short pulse for high core temperatures is likely to be at a higher intensity $\sim 10^{20}$ W/cm^2 to bring in more energy, but at a green or blue (if available) wavelength to better match the hot electron range to the core. We have also found that nesting a second, smaller cone inside the first and possibly filling it with low-density CH foam can produce smoother, better-focused hot electron deposition.

Conditions close to those in Kodama *et al.*'s cone target experiments have been examined with implicit ANTHEM. Core temperatures close to the experimental values are predicted for a range of plausible choices for resistivity, drag, spot shape, cone-core spacing, and intensity variations. Return current joule heating (not ''magnetic stopping'' [10]) accounts for the core heating. Spontaneously arising B fields lead to surface retention and filamentation of penetrating hot electrons. Shorter wavelength drive pulses are predicted to increase the core temperature and thus the neutron yield.

The author is grateful to Evan Dodd, Brian Albright, and Max Tabak for helpful discussions.

*Electronic address: rodmason01@msn.com

[1] M. Tabak *et al.*, Phys. Plasmas **1**, 1626 (1994).
[2] S. J. Clarke, H. N. Fisher, and R. J. Mason, Phys. Rev. Lett. **30**, 89 (1973); R. J. Mason and R. L. Morse, Phys. Fluids **18**, 814 (1975); R. J. Mason, Nucl. Fusion **15**, 1031 (1975).
[3] G. S. Fraley, E. J. Linnebur, R. J. Mason, and R. L. Morse, Phys. Fluids **17**, 474 (1974).
[4] R. Kodama *et al.*, Nature (London) **412**, 798 (2001); R. Kodama *et al.*, Nature (London) **418**, 933 (2002).
[5] R. B. Stephens *et al.*, Phys. Plasmas **12**, 056312 (2005); R. B. Stephens *et al.*, Phys. Rev. Lett. **91**, 185001 (2003).
[6] R. J. Mason, J. Comput. Phys. **71**, 429 (1987); R. J. Mason and C. W. Cranfill, IEEE Trans. Plasma Sci. **PS-14**, 45 (1986).
[7] R. J. Mason, J. Comput. Phys. **41**, 233 (1981); **51**, 484 (1983).
[8] S. C. Wilks *et al.*, Phys. Rev. Lett. **69**, 1383 (1992).
[9] R. J. Mason, E. S. Dodd, and B. J. Albright, Phys. Rev. E **72**, 015401 (2005).
[10] R. B. Campbell *et al.*, Phys. Rev. Lett. **94**, 055001 (2005).
[11] T. Mehlhorn (private communication).
[12] J. D. Jackson *Classical Electrodynamics* (Wiley, NY, 1975), 2nd ed., Chap. 13.
[13] Y. Sentoku, Phys. Rev. Lett. **90**, 155001 (2003).
[14] R. J. Mason, E. S. Dodd, B. J. Albright, in Proceedings of IFSA 2005 [J. Phys. IV (France) (to be published)].